

## Factors Affecting the Hydrogenation of Substituted Benzenes and Phenols over a Sulfided NiO–MoO<sub>3</sub>/γ-Al<sub>2</sub>O<sub>3</sub> Catalyst<sup>1</sup>

CLAUDINE AUBERT, ROBERT DURAND, PATRICK GENESTE, AND CLAUDE MOREAU

*Laboratoire de Chimie Organique Physique et Cinétique Chimique Appliquées, CNRS UA 418, Ecole Nationale Supérieure de Chimie de Montpellier, 8 rue Ecole Normale, 34075 Montpellier Cedex, France*

Received January 2, 1987; revised January 18, 1988

The hydrogenation of substituted benzenes ( $R = \text{Et, Ph, } c\text{-C}_6\text{H}_{11}, \text{PhCH}_2, c\text{-C}_6\text{H}_{11}\text{CH}_2$ ), of *ortho*- and *para*-substituted phenols ( $R = \text{Et, Ph, } c\text{-C}_6\text{H}_{11}, \text{PhCH}_2$ ) was studied by a batch method at 340°C and 70 bar H<sub>2</sub> over a sulfided NiO–MoO<sub>3</sub>/γ-Al<sub>2</sub>O<sub>3</sub> catalyst. The rates of hydrogenation are always higher for phenols than for benzenes and can be related to differences in the π-electron delocalization between the two series of organic compounds. The rates of hydrogenation of *ortho*- and *para*-substituted phenols are similar to one another and generally lower than those for phenol alone, thus suggesting a predominant role of electronic factors over steric ones. © 1988 Academic Press, Inc.

### INTRODUCTION

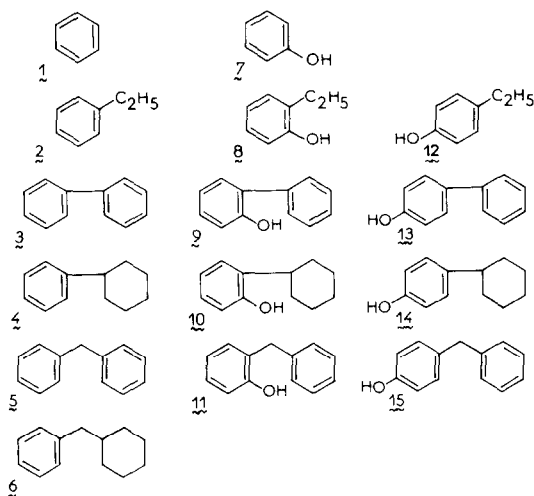
The replacement of light petroleum feedstocks by heavy oils, shale, or coal oils and the increasing demand for clean liquid fuels have led to a growth of catalytic cracking capacity. As a consequence, these heavy fossil fuels must be pretreated to prevent poisoning of cracking catalysts by S-, N-, or O-containing compounds. The principal catalytic reactions are referred to as hydrodesulfurization (HDS), hydrodenitrogenation (HDN), and hydrodeoxygenation (HDO) in which the removal of heteroatoms is in some cases accompanied by hydrogenation of aromatic rings. For sulfur-containing aromatic compounds, the C–S bond is always cleaved before any aromatic hydrogenation (1, 2), particularly in the thiophenol series. A different behavior is observed with nitrogen-containing aromatic compounds where hydrogenation of aromatic rings is generally required prior to C–N bond cleavage (1–3), particularly in the aniline series. For oxygen-containing

compounds, phenols behave like the nitrogen compounds; i.e., there is prior hydrogenation (2, 4), whereas a competition between hydrogenation and hydrogenolysis exists with phenolic ethers (2).

In these series and others where heteroatoms are included in aromatic systems, hydrogenation is therefore a key step in hydrotreatment reactions. Surprisingly, there has been little characterization of these reactions.

In recent papers (2–4) we have shown that organic reactant–catalyst interactions play an important role in the mechanism of removal of heteroatoms over a sulfided NiO–MoO<sub>3</sub>/γ-Al<sub>2</sub>O<sub>3</sub> catalyst and particularly in the hydrogenation step. As further investigations, we report now results on the hydrogenation of a series of substituted benzenes (1 to 6), a series of *ortho*-substituted phenols (7 to 11), and a series of *para*-substituted phenols (12 to 15) at 340°C and 70 bar H<sub>2</sub> over the same sulfided NiO–MoO<sub>3</sub>/γ-Al<sub>2</sub>O<sub>3</sub> as used in our previous studies (2, 4). Most of these compounds are present in the feedstocks but can also be considered as intermediates in hydroprocessing of heavier molecules.

<sup>1</sup> Part of this work was presented at the French–Venezuelan Symposium on Catalysis held in Rueil-Malmaison, France, 1985.



## EXPERIMENTAL

The catalyst used was Procatalyse HR 346, which has the following composition: 3% NiO, 14% MoO<sub>3</sub>, and 83% Al<sub>2</sub>O<sub>3</sub>. It was sulfided at atmospheric pressure using a fluidized-bed technique with a gas mixture of 15% H<sub>2</sub>S and 85% H<sub>2</sub> by volume. The catalyst was heated in flowing H<sub>2</sub>/H<sub>2</sub>S (gas flow, 120 ml/min) from 20 to 400°C (8°C/min) and held at 400°C for 4 h, then cooled, and finally swept with nitrogen for 30 min.

Experiments were carried out in a 0.3-liter stirred autoclave (Autoclave Engineers Type Magne-Drive), operating in a batch mode at 340°C and 70 bar of hydrogen pressure [see Ref. (2) for typical procedure].

Analyses were performed on a Girdel 30 gas chromatograph equipped with a flame ionization detector using hydrogen as carrier gas. Wall-coated open tubular fused silica capillary columns used were Chrompack CP Sil 5 CB(OV1) or CP Sil 19 CB(OV17), 10 m × 0.22 mm i.d. Products were identified by comparison with authentic samples and GC-MS analysis.

The rate constants were deduced from the experimental curves by curve fitting and simulation, assuming all the reactions to be first order in the organic reactant. The calculated reaction rate constants (in min<sup>-1</sup>) depend on the weight of catalyst and are then referred to 1 g of catalyst. The experi-

mental errors on the rate constants can be estimated at ±15%.

## RESULTS

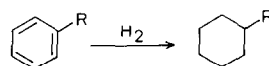
*Hydrogenation of Aromatic Hydrocarbons*

The reaction networks for hydrogenation of benzenes substituted by saturated or aromatic groups, ethyl (2), phenyl (3), cyclohexyl (4), benzyl (5) or cyclohexylmethyl (6) over a sulfided NiO-MoO<sub>3</sub>/γ-Al<sub>2</sub>O<sub>3</sub> catalyst at 340°C and 70 bar H<sub>2</sub> are given in Scheme 1. When the substituents are also subject to hydrogenation, the reaction proceeds through consecutive steps.

The first-order rate constants deduced from the experimental plots of concentrations against time are similar whatever the substituent and are given in Table 1.

The concentration vs time plot for hydrogenation of biphenyl (3) is given in Fig. 1. A similar plot was also obtained for hydrogenation of diphenylmethane (5). The curves drawn are computer-simulated, based on kinetic consecutive networks as given in Scheme 1.

As shown in Table 1, the presence of saturated groups such as ethyl (2) or bulkier ones like cyclohexyl (4), cyclohexylmethyl (6), or a second function capable of being hydrogenated like benzyl (5) does not significantly affect the rate of hydrogenation of a benzene ring. We can therefore exclude the intervention of steric factors in the processes of π-adsorption onto the cat-


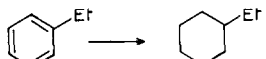
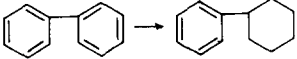
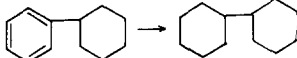
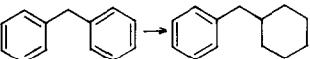
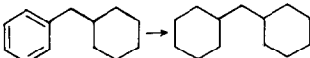


- 1 R = H
- 2 R = C<sub>2</sub>H<sub>5</sub>
- 3 R = C<sub>6</sub>H<sub>5</sub>
- 4 R = c-C<sub>6</sub>H<sub>11</sub>
- 5 R = C<sub>6</sub>H<sub>5</sub>-CH<sub>2</sub>
- 6 R = c-C<sub>6</sub>H<sub>11</sub>-CH<sub>2</sub>

SCHEME 1. Reaction network for hydrogenation of benzenes substituted by saturated or aromatics groups over sulfided NiO-MoO<sub>3</sub>/γ-Al<sub>2</sub>O<sub>3</sub> at 340°C and 70 bar H<sub>2</sub>.

TABLE I

Hydrogenation Rate Constants for Benzene and Substituted Benzenes at 340°C, 70 bar H<sub>2</sub> over sulfided NiO-MoO<sub>3</sub>/γ-Al<sub>2</sub>O<sub>3</sub> Catalyst

Organic reactant $\xrightarrow{k}$ product	$k^a$
	2
	2
	6
	2
	3
	2

<sup>a</sup> Rate constants  $\times 10^3 \text{ min}^{-1} \cdot (\text{g} \cdot \text{cat.})^{-1}$ .

alyst. Likewise, we can rule out the intervention of electronic factors which do not differ in a significant manner from one substituent to another (5).

When a second group capable of being

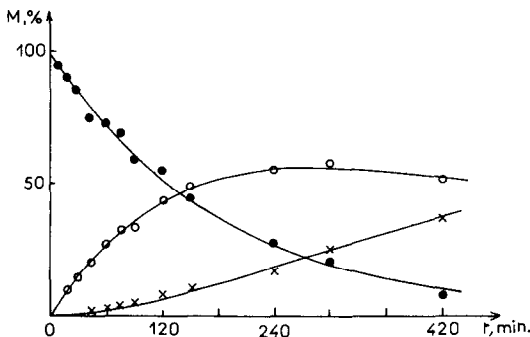


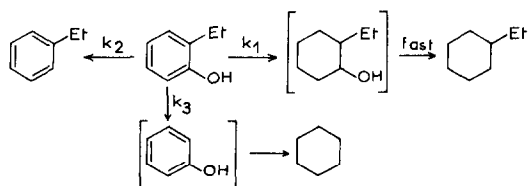
FIG. 1. Product distribution vs time for hydroprocessing of biphenyl over sulfided NiO-MoO<sub>3</sub>/γ-Al<sub>2</sub>O<sub>3</sub> at 340°C and 70 bar H<sub>2</sub>; biphenyl (●), cyclohexylbenzene (○), dicyclohexyl (×).

hydrogenated such as phenyl is directly bound to the benzene ring which undergoes hydrogenation as in the case of biphenyl (3), a slight exaltation of the rate of hydrogenation is observed on a supported NiO-MoO<sub>3</sub> catalyst whereas biphenyl behaves like benzene on a supported CoO-MoO<sub>3</sub> catalyst (6). This slight exaltation could result from some kind of "anchor effect" which is found again, to a lesser extent, in the increased hydrogenation rate of diphenylmethane (5). This occurs in spite of a loss of resonance due to steric interactions between the two aromatic rings preventing their coplanarity (7).

#### Hydrogenation of *ortho*- and *para*-Substituted Phenols

*Phenol* (7). As already reported in a previous paper (2), the hydrogenation of phenol (7) mainly yields cyclohexane through the formation of intermediate cyclohexanol. The percentage of hydrogenolysis of the C-OH bond leading to benzene was estimated at about 5%.

*ortho*-Ethylphenol (8) and *para*-ethylphenol (12). As for phenol, the hydroprocessing of *ortho*-ethylphenol (8) over the sulfided NiO-MoO<sub>3</sub>/γ-Al<sub>2</sub>O<sub>3</sub> catalyst gives ethylcyclohexane as the major product through hydrogenation of the phenolic ring (Scheme 2,  $k_1$ ). Small amounts of ethylbenzene resulting from hydrogenolysis of the C-OH bond ( $\approx 5\%$ , Scheme 2,  $k_2$ ) and cyclohexane resulting from cleavage of the C-ethyl bond ( $\approx 10\%$ , Scheme 2,  $k_3$ ) are also observed. The concentration vs time plots for *ortho*-ethylphenol hydroprocessing are given in Fig. 2. The curves drawn in



SCHEME 2. Reaction network for hydroprocessing of *ortho*-ethylphenol over sulfided NiO-MoO<sub>3</sub>/γ-Al<sub>2</sub>O<sub>3</sub> at 340°C and 70 bar H<sub>2</sub>.

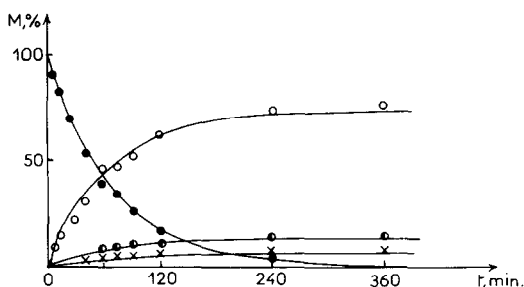


FIG. 2. Product distribution vs time for hydroprocessing of *ortho*-ethylphenol over sulfided NiO-MoO<sub>3</sub>/γ-Al<sub>2</sub>O<sub>3</sub> at 340°C and 70 bar H<sub>2</sub>; *ortho*-ethylphenol (●), ethylcyclohexane (○), ethylbenzene (×), cyclohexane (●).

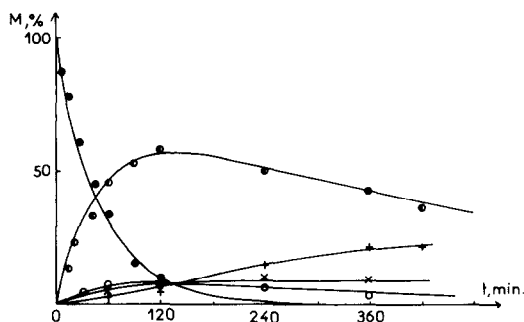


FIG. 3. Product distribution vs time for hydroprocessing of *ortho*-phenylphenol over sulfided NiO-MoO<sub>3</sub>/γ-Al<sub>2</sub>O<sub>3</sub> at 340°C and 70 bar H<sub>2</sub>; *ortho*-phenylphenol (●), cyclohexylbenzene (○), biphenyl (●), dicyclohexyl (+), cyclohexane (×).

Fig. 2 are computer-simulated based on the parallel reaction network shown in Scheme 2.

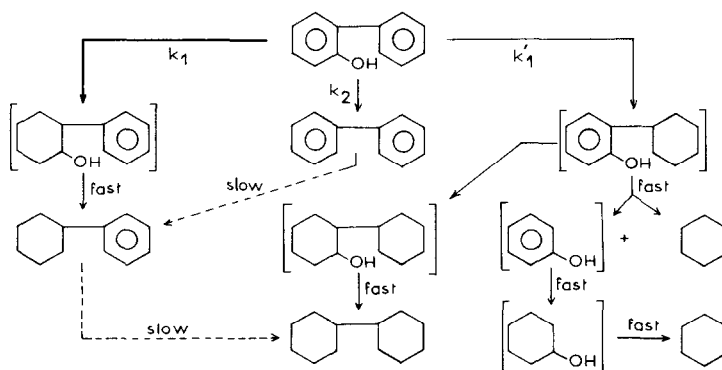
The values of the rate constants resulting from Scheme 2 are the following:  $k_1 = 12 \times 10^{-3}$ ,  $k_2 = 1 \times 10^{-3}$ , and  $k_3 = 2 \times 10^{-3} \text{ min}^{-1} \cdot (\text{g} \cdot \text{cat.})^{-1}$  at 340°C and 70 bar H<sub>2</sub>.

*para*-Ethylphenol (12) behaves like *ortho*-ethylphenol with  $k_1 = 12 \times 10^{-3} \text{ min}^{-1} \cdot (\text{g} \cdot \text{cat.})^{-1}$ .

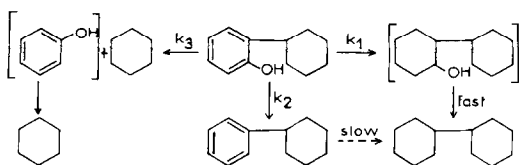
*ortho*-Phenylphenol (9) and *para*-phenylphenol (13). The hydrodeoxygenation of *ortho*-phenylphenol (9), an identified intermediate in the hydroprocessing of dibenzofuran, yields cyclohexylbenzene through hydrogenation of the phenolic ring (Scheme 3,  $k_1$ ), dicyclohexyl and cyclohexane through hydrogenation of the phenyl ring

(Scheme 3,  $k'_1$ ) and biphenyl through hydrogenolysis of the phenolic C-OH bond (Scheme 3,  $k_2$ ). Plots of concentration vs time are given in Fig. 3. The rate constants deduced from these plots by curve fitting according to the reaction network given in Scheme 3 are the following:  $k_1 = 14 \times 10^{-3}$ ,  $k'_1 = 2 \times 10^{-3}$ , and  $k_2 = 2 \times 10^{-3} \text{ min}^{-1} \cdot (\text{g} \cdot \text{cat.})^{-1}$ .

From these results, it can be seen that the formation of cyclohexylbenzene through the hydrogenation of the phenol moiety of *ortho*-phenylphenol ( $k_1$ , Scheme 3) is largely favored over the other steps and particularly over the hydrogenation of the phenyl moiety of *ortho*-phenylphenol ( $k'_1$ , Scheme 3).



SCHEME 3. Reaction network for hydroprocessing of *ortho*-phenylphenol over sulfided NiO-MoO<sub>3</sub>/γ-Al<sub>2</sub>O<sub>3</sub> at 340°C and 70 bar H<sub>2</sub>.



SCHEME 4. Reaction network for hydroprocessing of *ortho*-cyclohexylphenol over sulfided NiO–MoO<sub>3</sub>/γ-Al<sub>2</sub>O<sub>3</sub> at 340°C and 70 bar H<sub>2</sub>.

Another characteristic feature of HDO of phenols over sulfided NiO–MoO<sub>3</sub>/γ-Al<sub>2</sub>O<sub>3</sub> is the high percentage of hydrogenation as compared to hydrogenolysis, 90% for phenol itself (2); a similar behavior is also observed in the hydrodeoxygenation of *ortho*-phenylphenol where the rate ratio hydrogenation/hydrogenolysis ( $k_1 + k'_1/k_2$ , Scheme 3) is nearly the same.

The rate of hydrogenation of the phenolic ring of *para*-phenylphenol (13) under the same experimental conditions does not differ from that of the *ortho* isomer ( $17 \times 10^{-3} \text{ min}^{-1} (\text{g} \cdot \text{cat.})^{-1}$  for the former and  $14 \times 10^{-3} \text{ min}^{-1} (\text{g} \cdot \text{cat.})^{-1}$  for the latter).

*ortho*-Cyclohexylphenol (10) and *para*-cyclohexylphenol (14). The hydroprocessing of *ortho*-cyclohexylphenol (10) over a sulfided NiO–MoO<sub>3</sub>/γ-Al<sub>2</sub>O<sub>3</sub> catalyst mainly yields dicyclohexyl through hydrogenation of the phenolic ring (Scheme 4,  $k_1$ ) and cyclohexane through cracking of the α-C–C bond (Scheme 4,  $k_3$ ); a small quantity of cyclohexylbenzene is observed, resulting from the cleavage of the phenolic C–OH bond (Scheme 4,  $k_2$ ). Plots of concentration vs time are given in Fig. 4 for HDO of *ortho*-cyclohexylphenol.

The experimental curves plotted in Fig. 4 result from the kinetic reaction network shown in Scheme 4, with  $k_1 = 24 \times 10^{-3}$ ,  $k_2 = 6 \times 10^{-3}$ , and  $k_3 = 20 \times 10^{-3} \text{ min}^{-1} \cdot (\text{g} \cdot \text{cat.})^{-1}$  at 340°C and 70 bar H<sub>2</sub>. It can thus be seen that the cleavage of the C–cyclohexyl bond is as important as the hydrogenation of the phenolic ring for HDO of *ortho*-phenylcyclohexanol. It should also be noted that this cleavage between the two rings does not occur in HDO of 2-phenylcy-

clohexanol (see Scheme 3); these points are detailed later in the discussion.

As for *ortho*-cyclohexylphenol, a similar behavior is observed for HDO of *para*-cyclohexylphenol (14) with a rate constant for the hydrogenation of the phenolic ring equal to  $25 \times 10^{-3} \text{ min}^{-1} \cdot (\text{g} \cdot \text{cat.})^{-1}$ .

*ortho*-Benzylphenol (11) and *para*-benzylphenol (15). The hydrodeoxygenation of *ortho*-benzylphenol (11), a postulated intermediate in the overall hydroprocessing of xanthene, over sulfided NiO–MoO<sub>3</sub>/γ-Al<sub>2</sub>O<sub>3</sub> catalyst yields phenylcyclohexylmethane through hydrogenation of the phenolic ring (Scheme 5,  $k_1$ ), toluene and cyclohexane through cracking of the α-C–C bond (Scheme 5,  $k_3$ ), and methylcyclohexane and benzene through cracking of the β-C–C bond (Scheme 5,  $k'_3$ ). Small amounts of diphenylmethane resulting from hydrogenolysis of the phenolic C–OH bond (Scheme 5,  $k_2$ ) and dicyclohexylmethane are also detected. The concentration vs time plots for *ortho*-benzylphenol hydroprocessing are given in Fig. 5. The curves drawn in Fig. 5 are computer-simulated, based on the reaction network given in Scheme 5. The individual rate constants of the different steps are the following at 340°C and 70 bar H<sub>2</sub>:  $k_1 = 25 \times 10^{-3}$ ,  $k_2 = 2 \times 10^{-3}$ ,  $k_3 = 65 \times 10^{-3}$ , and  $k'_3 = 15 \times 10^{-3} \text{ min}^{-1} \cdot (\text{g} \cdot \text{cat.})^{-1}$ .

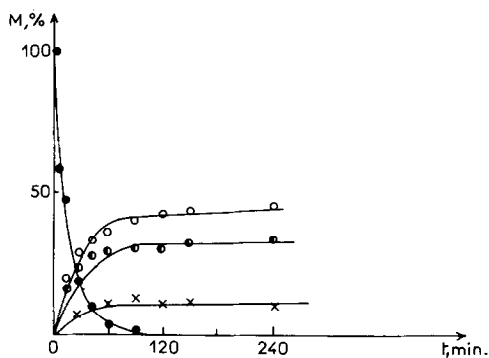
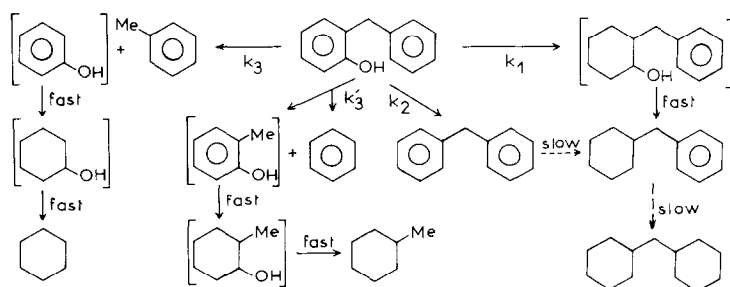


FIG. 4. Product distribution vs time for hydroprocessing of *ortho*-cyclohexylphenol over sulfided NiO–MoO<sub>3</sub>/γ-Al<sub>2</sub>O<sub>3</sub> at 340°C and 70 bar H<sub>2</sub>; *ortho*-cyclohexylphenol (●), dicyclohexyl (○), cyclohexylbenzene (×), cyclohexane (◐).



SCHEME 5. Reaction network for hydroprocessing of *ortho*-benzylphenol over sulfided NiO–MoO<sub>3</sub>/ $\gamma$ -Al<sub>2</sub>O<sub>3</sub> at 340°C and 70 bar H<sub>2</sub>.

From these results it can be seen that the formation of phenylcyclohexylmethane through the hydrogenation of the phenolic moiety of *ortho*-benzylphenol ( $k_1$ , Scheme 5) is largely favored over the formation of diphenylmethane through the hydrogenolysis of the C–O bond ( $k_2$ , Scheme 5). This behavior has already been considered in HDO of other *ortho*-substituted phenols.

The important feature to be noted is the predominant C–C bond scission ( $k_3$  and  $k_3'$ , Scheme 5). It is well known that the dissociation energy of a benzylic C–C bond (234 kJ/mol for bibenzyl) is considerably lower than that of a benzenic C–C bond (485 kJ/mol for biphenyl) ( $\delta$ ) and this difference is sufficient to account for the high degree of cracking in HDO of *ortho*-benzylphenol. It should also be noted that diphenylmethane itself, like biphenyl, is not subject to C–C bond cleavage under the same experimental conditions.

As for the preceding *para*-substituted phenols, *para*-benzylphenol (**15**) behaves like its *ortho* isomer with a rate constant for the hydrogenation of the phenolic ring equal to  $17 \times 10^{-3} \text{ min}^{-1} \cdot (\text{g} \cdot \text{cat.})^{-1}$ .

The rate constants for the hydrogenation of the phenolic rings of phenol and *ortho*- and *para*-substituted phenols are summarized in Table 2. These results provoke the following comments. (i) From a comparison of Tables 1 and 2 it can be seen that phenols

TABLE 2

Hydrogenation Rate Constants for Phenol, *ortho*-Substituted Phenols, and *para*-Substituted Phenols at 340°C, 70 bar H<sub>2</sub> over Sulfided NiO–MoO<sub>3</sub>/ $\gamma$ -Al<sub>2</sub>O<sub>3</sub> Catalyst

Organic reactant $\xrightarrow{k}$ product	$k_{ortho}^a$	$k_{para}^a$
	33	
	12	12
	14	17
	24	25
	25	17

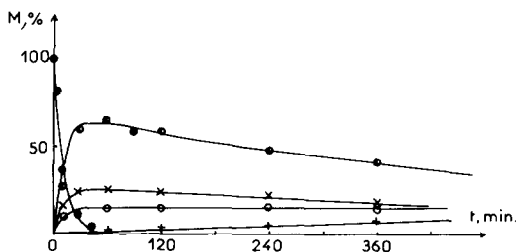


FIG. 5. Product distribution vs time for hydroprocessing of *ortho*-benzylphenol over sulfided NiO–MoO<sub>3</sub>/ $\gamma$ -Al<sub>2</sub>O<sub>3</sub> at 340°C and 70 bar H<sub>2</sub>; *ortho*-benzylphenol (●), toluene + cyclohexane (○), phenylcyclohexylmethane (×), methylcyclohexane + benzene (○), dicyclohexylmethane (+).

<sup>a</sup> Rate constants  $\times 10^3 \text{ min}^{-1} \cdot (\text{g} \cdot \text{cat.})^{-1}$ . Abbreviations: Et, ethyl; Ph, phenyl; *c*-C<sub>6</sub>H<sub>11</sub>, cyclohexyl; and Bz, benzyl.

are more rapidly hydrogenated than their parent aromatic hydrocarbons whatever the position of substituents. (ii) The presence of substituents at the *ortho* position leads to a slight decrease in the rate of hydrogenation of *ortho*-substituted phenols on sulfided NiO–MoO<sub>3</sub>/γ-Al<sub>2</sub>O<sub>3</sub> catalyst. A similar behavior was also observed by Rollmann (9) on a sulfided CoO–MoO<sub>3</sub>/γ-Al<sub>2</sub>O<sub>3</sub> catalyst for phenols (8) and (9). The lower reactivity of alkyl O- and S-substituted heteroaromatics was rationalized by Rollmann (9) and Houalla *et al.* (10) as due to increased steric hindrance at the *ortho* position. We can add that this alkyl *ortho* effect is also working in the hydrodenitrogenation of *ortho*-ethylaniline and *ortho*, *ortho*'-diethylaniline as compared to aniline on sulfided NiO–WO<sub>3</sub>/γ-Al<sub>2</sub>O<sub>3</sub> catalysts (11) as well as on sulfided NiO–MoO<sub>3</sub>/γ-Al<sub>2</sub>O<sub>3</sub> (3). This steric hindrance was also thought to be associated with entropic considerations as reported by Odeunmi and Ollis in the hydrodeoxygenation of cresols on a sulfided CoO–MoO<sub>3</sub>/γ-Al<sub>2</sub>O<sub>3</sub> catalyst (12).

The origin of the *ortho* effect was recently reviewed (13, 14) and the authors concluded that steric effects are not significant for *ortho*-phenols, *ortho*-anilines, or *ortho*-pyridines; thus the *ortho* effect would seem rather to be electronic in nature. This hypothesis is easily verified by comparing the reactivities of *ortho*- and *para*-phenols which are electronically identical so that, if steric effects were present, they would appear with the *ortho* isomer and not with the *para* isomer. As seen in Table 2, *ortho*- and *para*-substituted phenols are hydrogenated at similar rates and the slight rate decrease cannot therefore be accounted for in terms of steric hindrance.

#### DISCUSSION

##### *Hydrogenation of Aromatic Hydrocarbons and Phenols*

Phenols are more rapidly hydrogenated than their corresponding hydrocarbons and

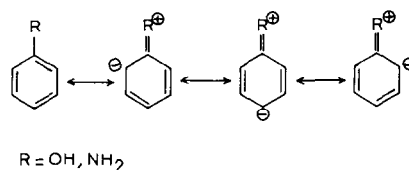


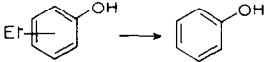
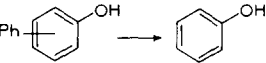
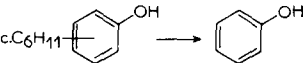
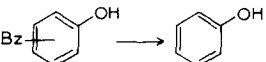
FIG. 6. Resonance effects caused by OH or NH<sub>2</sub> groups.

we have shown in previous papers (2, 4) that the reactivities could be related to differences in the strength of adsorption between the adsorbed state and the transition state. In the present work, this would imply a more stabilized adsorbed state with benzenes than with phenols, thus increasing the energy differences between the adsorbed state and the transition state. In other words the binding strength between the organic reactant and the catalyst should be more important for benzene than for phenol or aniline. This assumption seems to be valid as the  $\pi$ -system is completely delocalized in the former case whereas the presence of polar groups like OH or NH<sub>2</sub> implies charges localized at preferred positions (Fig. 6) leading to a diminution of the strength of the  $\pi$ -adsorption and to higher reaction rates.

The presence of substituents at the *ortho* position of phenols generally leads to a lower reactivity as compared to phenol alone. This rate decrease is also observed for *para* substituents, thus ruling out the influence of steric factors on the reactivity. The *ortho* effect must rather depend on electronic effects (inductive and mesomeric effects) and, more precisely, must result from a change in the  $\sigma$ -charge distribution leading to a reduced  $\pi$ -donation to the ring at the *ortho* position and, to a smaller extent, at the *para* position (15). On this basis, the delocalization of the  $\pi$ -system would be modified in such a manner that the binding force between the organic reactant and the catalyst should be stronger with  $\sigma$ -electron-donating substituents than with  $\sigma$ -electron-withdrawing ones, thus reducing the  $\pi$ -donation to the system.

TABLE 3

Substituent C-C Bond Cleavage Rate Constants for *ortho*- and *para*-Substituted Phenols at 340°C, 70 bar H<sub>2</sub> over Sulfided NiO-MoO<sub>3</sub>/γ-Al<sub>2</sub>O<sub>3</sub> Catalyst

Organic reactant $\xrightarrow{k}$ product	C-C bond cleavage (%)	$k^a$
	5	2
	—	—
	40	20
	80	65

<sup>a</sup> Rate constants  $\times 10^3 \text{ min}^{-1} \cdot (\text{g} \cdot \text{cat.})^{-1}$ . Abbreviations: see Table 2.

#### Cleavage of Substituent C-C Bonds

As reported in Table 3, phenols substituted by ethyl, cyclohexyl, or benzyl groups at the *ortho* and *para* positions may also undergo cleavage of C-C bonds, whereas the corresponding hydrocarbons are inactive under the same experimental conditions. The percentage of cleavage increases from ethyl to benzyl, thus following the order of reactivity observed in both cracking (16) and hydrocracking (17) reactions, implying formation of carbocations, the most stabilized being the tropylium ion C<sub>6</sub>H<sub>5</sub>-CH<sub>2</sub><sup>+</sup>. This could also be related to the ease of cleavage of C-C bonds as mentioned earlier for benzylic C-C bonds as compared to benzenic C-C bonds; the higher energy of dissociation observed for the latter case would thus account for the absence of cleavage of the C-C bond for the biphenyl system because of the stabilization of this system through resonance.

As for hydrogenation, C-C bond cleavages are also strongly influenced by electronic properties, particularly by the electron-donating ability of OH groups through

resonance. Neutral groups like alkyl, phenyl, or aryl do not allow cleavage of C-C bonds under the experimental conditions reported in this paper.

#### CONCLUSIONS

The main conclusions which can be drawn from this work on the hydrogenation of aromatic hydrocarbons and hydrodeoxygenation of *ortho*- and *para*-substituted phenols over a sulfided NiO-MoO<sub>3</sub>/γ-Al<sub>2</sub>O<sub>3</sub> catalyst are the following.

(i) The hydrogenating activity is closely dependent on the aromaticity of the system to be hydrogenated through the more or less important delocalization of  $\pi$ -electrons resulting from the electron-donating ability of OH or NH<sub>2</sub> groups by resonance (18).

(ii) The lower reactivity observed for hydrogenation of *ortho*- and *para*-substituted phenols than that of phenol itself would appear to result from electronic effects rather than steric ones.

(iii) The hydrocracking activity observed during the course of hydroprocessing of phenols is still dependent on the aromatic character of the system and  $\pi$ -electron delocalization.

It is thus clear that aromaticity associated with a greater or lesser  $\pi$ -electron delocalization is mainly responsible for the reactivity of aromatic hydrocarbons and substituted phenols (this work), substituted anilines (11), and pyridine-like compounds (19).

#### REFERENCES

- For recent reviews on hydrotreating reactions, see Schulz, H., Schon, M., and Rahman, N. M., "Studies in Surface Science and Catalysis," Vol. 27, p. 201. Elsevier, Amsterdam, 1986, and references therein; Zdražil, M., and Kraus, M., "Studies in Surface Science and Catalysis," Vol. 27, p. 257. Elsevier, Amsterdam, 1986, and references therein.
- Aubert, C., Durand, R., Geneste, P., and Moreau, C. *J. Catal.* **97**, 169 (1986).
- Olivé, J. L., Biyoko, S., Moulinas, C., and Geneste, P., *Appl. Catal.* **19**, 165 (1985).



4. Aubert, C., Durand, R., Geneste, R., and Moreau, C., *Bull. Soc. Chim. Belg.* **93**, 653 (1984).
5. Exner, O., in "Correlation Analysis in Chemistry: Recent Advances" (N. B. Chapman and J. Shorter, Eds.), p. 500. Plenum, New York, 1978.
6. Sapre, A. V., and Gates, B. C., *Ind. Eng. Chem. Process. Des. Dev.* **20**, 68 (1981).
7. Merkel, E., and Wiegand, C., *Z. Naturforsch. B* **3**, 93 (1948).
8. Schlosberg, R. H., Szajowski, P. F., Dupre, G. D., Danik, J. A., Kurs, A., Ashe, T. R., and Olmstead, W. N., *Fuel* **62**, 690 (1983).
9. Rollman, L. D., *J. Catal.* **46**, 243 (1977).
10. Houalla, M., Broderick, D. H., Sapre, A. V., Nag, N. K., De Beer, V. H. J., Gates, B. C., and Kwart, H., *J. Catal.* **61**, 523 (1980).
11. Zmimita, N., Doctorat thesis, Montpellier, 1987.
12. Odebunmi, E. O., and Ollis, D. F., *J. Catal.* **80**, 56 (1983).
13. Fujita, T., *Prog. Phys. Org. Chem.* **14**, 75 (1983).
14. Gallo, R., *Prog. Phys. Org. Chem.* **14**, 115 (1983).
15. Mehler, E. L., and Gerhards, J., *J. Amer. Chem. Soc.* **107**, 5856 (1985).
16. Germain, J. E., "Catalytic Conversion of Hydrocarbons," p. 207. Academic Press, San Diego/London, 1969.
17. Weisser, O., and Landa, S., "Sulphide Catalysts, Their Properties and Applications," p. 134. Pergamon, Oxford, 1973.
18. Moreau, C., Bachelier, J., Bonnelle, J. P., Breyssse, M., Cattenot, M., Cornet, D., Decamp, T., Duchet, J. C., Durand, R., Engelhard, P., Frety, R., Gachet, C., Geneste, P., Grimblot, J., Gueguen, C., Kasztelan, S., Lacroix, M., Lavalley, J. C., Leclercq, C., de Mourgues, L., Olivé, J. L., Payen, E., Portefaix, J. L., Toulhoat, H., and Vrinat, M., *Amer. Chem. Soc. Div. Pet. Chem. Prepr.* **32**, 298 (1987).
19. Aubert, C., Durand, R., Geneste, P., Moreau, C., and Zmimita, N., *Acta Simp. Iberoam. Catal.*, 10th, 1153 (1986). Soc. Iberoam. Catal., Merida, Venezuela.